ELSEVIER

Robotics and Autonomous Systems 40 (2002) 267–277

Robotics and Autonomous Systems

www.elsevier.com/locate/robot

Modelling and calibration of the laser beam-scanning triangulation measurement system

Guoyu Wang [a,*], Bing Zheng [a], Xin Li [a], Z. Houkes [b,*,1], P.P.L. Regtien [b]

[a] *Department of Electrical Engineering, Ocean University of Qingdao, 266003 Qingdao, PR China*
[b] *Department of Electrical Engineering, University of Twente, 7500 AE Enschede, The Netherlands*

Received 29 August 2001; received in revised form 15 February 2002
Communicated by T.C. Henderson

Abstract

We present an approach of modelling and calibration of an active laser beam-scanning triangulation measurement system. The system works with the pattern of two-dimensional beam-scanning illumination and one-dimensional slit-scanning detection with a photo-multiplier tube instead of a CCD camera. By modelling the system-fixed coordinate, we describe the formulation of 3D computation and propose a calibration method in terms of LSE using a planar fitting algorithm. As a sensor-dependent solution, the estimation is refined in the domain of sensing variables. Result of calibration of the real system and a brief analysis of systematic errors are given.

Keywords: Laser scanning; Triangulation measurement; Calibration; Planar fitting

1. Introduction

Since the range images provide 3D data of the scene directly, they have been extensively used in autonomous systems as a powerful modality for 3D interpretation. There exist a multitude of range sensing systems designed for various applications with different sensing techniques [2–4,10–12]. In general, optical ranging techniques can be divided into two types: monocular and binocular systems. The monocular approaches are based on the propagation time of light, i.e., "time-of-flight" (TOF). The binocular approaches are in fact based on the "triangulation" technique. It uses controlled light, so-called "structured light", by which the correspondence between projection and sensing has been pre-defined. Thus the distance can be measured with the well-known triangulation algorithm. At moderate ranges, triangulation systems perform accurate and fast measurement and are easy to implement [2,11], so they are quite popular for 3D measurements.

In a triangulation measurement system, the controlled light pattern can be a set of points, lines or grids, etc., combined with a specific sensing configuration. The illuminating pattern and the mode of light detection determine the formulation of 3D measurement. The commonly reported laser-scanning ranging system used the strips or slits illumination pattern (typically created from a cylindrical lens) with a one-dimensional scanning procedure and CCD camera as the detector (e.g. [4,12]). However, light pattern

* Corresponding author. Tel.: +86-532-2032966; fax: +86-532-2032799 (G. Wang) Tel.: +31-74-267-2960; fax: +31-74-267-2900 (Z. Houkes).
E-mail addresses: gywang@mail.ouqd.edu.cn (G. Wang), z.houkes@el.utwente.nl (Z. Houkes).
[1] Tel.: +31-53-489-2790; fax: +31-53-489-1067.

0921-8890/02/$ – see front matter © 2002 Elsevier Science B.V. All rights reserved.
PII: S0921-8890(02)00247-6

can also be a set of points, directly projected by the laser beam onto the target (so-called "flying-point" scanning way). In this beam-scanning mode, although a two-dimensional scan mechanism is required, it shows advantages of high intensity in illumination and less back scattering in detection. This paper introduces an example of the laser-scanning triangulation system working with beam-scanning mode. Specifically, the detector of the sensing system is implemented with a photo-multiplier tube instead of CCD modality. Therefore, formulation of 3D measurement is not derived from the CCD image geometry, but calculated in a time-sequence way. Consequently, modelling and calibration of the system is different to those existing approaches in literature.

In a broad sense, calibration of a measuring system is to formalize data representation under a defined coordinate system. The focus of a calibration is to determine the system parameters that are involved in the computation of the output data. A variety of calibration methods have been presented [1,4–8,11,12,14]. However, no available calibration routines can be directly applied to the beam-scanning system introduced in this paper because the new features of the system induce new definitions in model of the measurement. Based on the example of the beam-scanning laser triangulation system, this paper introduces a new approach for calibration of the parameters of the measurement system. Commonly, a difficulty in calibration is the point correspondence between the predefined coordinate and the image coordinate [6,12]. Without CCD camera, we proposed a new algorithm to solve the point correspondence problem in parameter estimation. Through a planar fitting scheme, the system parameters are determined within an optimal framework. Moreover, the estimation is given with a sensor-dependent approach, by which the uncertainties in sensing processing are processed with a refined statistical model.

2. The working principles of the laser beam-scanning triangulation measurement system

Fig. 1 illustrates the principle of the laser beam-scanning triangulation measurement system. **F** denotes the laser emitter and **S** denotes the detector.

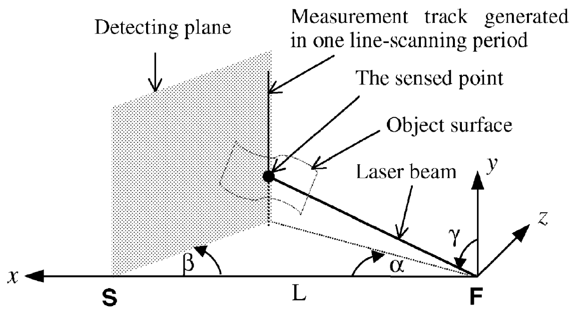

Fig. 1. Illustration of the measurement track. The laser is emitted from **F** and the slit-shaped detector is located at **S**. In one line-scanning period, the intersection of the laser beam and the detecting plane forms a near straight line along with y-axis, the so-called "measurement track". Intersection of this track and the object surface is just the sensed point. In one frame-scanning period, a number of measurement tracks are generated sequentially, each of which corresponding to different line-scanning routine.

L is the distance between these components, and is called the baseline. The laser beam performs scans in longitudinal direction (denoted as *line* scanning), and latitudinal direction (called *frame* scanning). A slit in front of the detector is projected onto the scene by a rotating mirror, so an imaged "detecting plane" thus scans in latitudinal direction (called *slit* scanning), whose angle β can be positioned while keeping the field-of-view in a fixed longitudinal direction. For any angle β, all visible illuminated object points on this detecting plane will be sensed. The frequency of the line scanning with respect to γ is much higher than that of the frame scanning with respect to α and the slit scanning with respect to β. So during one line-scanning period, the track of the laser beam projected on the detecting plane is almost a straight line perpendicular to the x–z plane. Only points on this track can be sensed by the detector. Thus one frame-*scanning* period contains a number of line-scanning periods, resulting in a set of sequential tracks moving along the depth direction (z-axis). All sensed points are the intersecting points of these tracks and the object surface.

Obviously, to obtain the visible data points overall the object surface in the view of field, the trace of tracks should move at latitudinal direction in different frame-scanning period. This can be done by consequently changing the initial position of the detecting plane in each frame-scanning period. In [15], moving

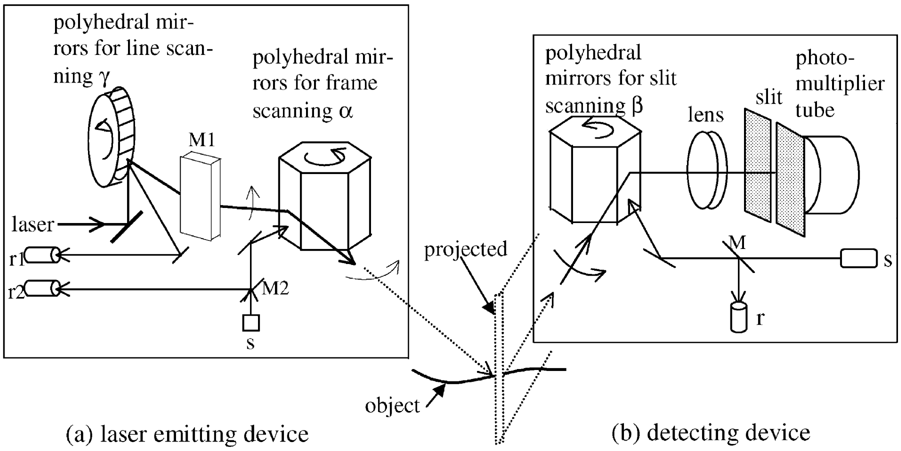

Fig. 2. Implementations of optical scanning and sensing scheme. (a) Illustrates line- and frame-scanning implementation. M1 is a fixed mirror transforming line scanning to frame scanning. The synchronizing signal for line scanning is generated by laser reflection at a certain pose of the mirror, detected by detector r1, while the synchronizing signal for frame scanning is generated also by reflected light at a defined position of the frame-scanning mirror, but an active illuminating source s is used. M2 is a semitransparent mirror by which reflected light is detected by r2. (b) Illustrates the slit-scanning implementation. A slit positioned at the focus of a lens is imaged onto space through the lens and the slit-scanning mirror. Then an imaged "detecting plane" is scanned using the mirror rotation. Only diffusion of the point that lies on the detecting plane can be sensed by the sensor behind the slit. The synchronizing signal is generated by illuminating source s and a detector r, coupled by the semitransparent mirror M.

of the tracks was controlled by setting a difference between the frequencies of the slit scanning and the frame scanning, so the measurement in overall working space can process automatically.

Particular in this system is that a photo-multiplier tube was used as the sensing modality instead of the commonly used CCD camera. This is to improve the *visibility* of the optical sensing system [15] because this 3D measurement system was basically designed for robotic inspection in underwater engineering tasks where the dark environment allows the feasibility of high-sensitivity photo-electronic elements. Therefore, sensing of object points is finished by the recording the three angles α, β and γ through a time sequential way. Setting the three scanning frequencies with respect to α, β and γ, the values of the three angles are then determined by the time recording with a synchronising mechanism to trigger the beginnings of each scanning period. More details about the construction of the laser beam-scanning measurement system were described in [13,15].

Fig. 2 shows a sketch of the implementation. The line and frame scanning were implemented with two orthogonal rotating mirrors by which the reflected laser beam runs in a two-dimensional scanning way as shown in Fig. 2(a). The detection device is mechanically independent to the laser-emanating device. A slit in front of the photo-multiplier tube is located at the focus of a lens so that a scanning "detecting plane" is generated in the scene. Scanning of the detecting plane is also carried out by a mirror-faced rotating polyhedron as shown in Fig. 2(b).

3. Modelling the triangulation measurement system

The model of 3D measurement is shown in Fig. 3. Suppose the laser beam originates from a fixed point **F** (laser-emanating origin) and scans along longitude and latitude directions by line and frame scanning. We define **F** to be the origin of the measuring coordinate system and the *y*-axis being perpendicular to the frame-scanning plane (denoted by Γ). During the sensing process, the detecting plane, denoted by Ψ, scans the space by rotating around a fixed axis whose direction is represented by the unit vector $\mathbf{n}_s$. Suppose $\mathbf{n}_s$ and the frame-scanning plane Γ intersect at point

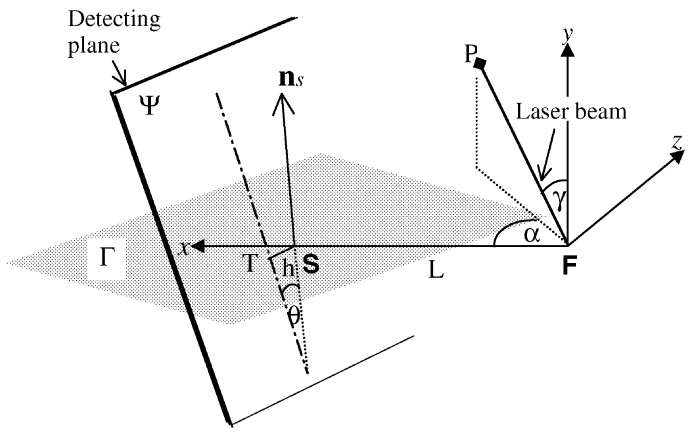

Fig. 3. Model of the coordinate system. $\mathbf{n}_\mathrm{s}$ is the direction vector of rotation axis of Ψ (the normal vector of plane Γ), h the distance of **S** to Ψ, θ the angle between $\mathbf{n}_\mathrm{s}$ and Ψ and L the baseline between **S** and **F**.

S, then the x-axis of the measuring coordinate system is defined along **FS**. Having defined the x- and y-axes, the z-axis follows according to the right-hand rule. The distance between **F** and **S**, denoted by L, is the baseline length.

It should be noted that in this model the rotation axis $\mathbf{n}_\mathrm{s}$ of the detecting plane Ψ is assumed to be free-oriented with respect to the y-axis, the rotation axis of the laser frame scanning. The detecting plane Ψ is also assumed to be arbitrarily posed without any mechanical constraints. This freedom in the definition of a coordinate system is important because in practice, it is difficult to guarantee some mechanical constraints even there are intentions to do so.

There are four parameters to configure the pose of $\mathbf{n}_\mathrm{s}$ and Ψ. Two are used to describe the orientation of $\mathbf{n}_\mathrm{s}$, i.e., azimuth ρ_1 and elevation ρ_2 (see Fig. 5) with respect to the x–y–z coordinate system. Another two parameters describe the relative pose of the detecting plane Ψ with respect to $\mathbf{n}_\mathrm{s}$, i.e., the angle between $\mathbf{n}_\mathrm{s}$ and plane Ψ, denoted by θ, and the distance from point **S** to plane Ψ, denoted by h (see Fig. 3). These four parameters are independent of the scanning process. In summary, the parameters involved in a 3D measurement in the defined coordinate system are:

- α_0, β_0 and γ_0—three initial angles of the periodic scanning for α, β and γ.
- ρ_1 and ρ_2—azimuth and elevation angles describing the orientation of the vector $\mathbf{n}_\mathrm{s}$ referred to the x–y–z coordinates.
- h—distance between **S** and the detecting plane Ψ.
- θ—angle between the plane Ψ and $\mathbf{n}_\mathrm{s}$.
- L—baseline determined by the distance between **S** and **F**.

The 3D coordinate computation is derived from the simple fact that the sensed point is just the intersecting point of the laser beam and the detecting plane. Suppose the point P (see Fig. 3) is sensed at the recorded times indicated as t_f, t_l and t_s, with respect to the frame scanning, line scanning and slit scanning. Given t_f and t_l, the line equation of the laser beam is directly available in x–y–z coordinates from the known α and γ in the form:

$$\mathbf{x} = K \begin{bmatrix} \cos\alpha\sin\gamma \\ \cos\gamma \\ \sin\alpha\sin\gamma \end{bmatrix} = K\mathbf{q}. \tag{1}$$

Once the equation for the plane Ψ is formulated in the x–y–z coordinate system, the position of the point P expressed in the x–y–z coordinate system is determined by solving these two equations.

In order to obtain the equation of the detecting plane Ψ in the x–y–z coordinate system, an assistant coordinate system with origin at **S** is defined to describe the pose of Ψ when scanning. This assistant coordinate system, denoted as x'–y'–z', is built as described below.

Perpendicular to the rotation axis $\mathbf{n}_\mathrm{s}$ and passing through the point **S**, a so-called "scanning plane" is defined, which is denoted as Γ (shown in Fig. 3 as shad-

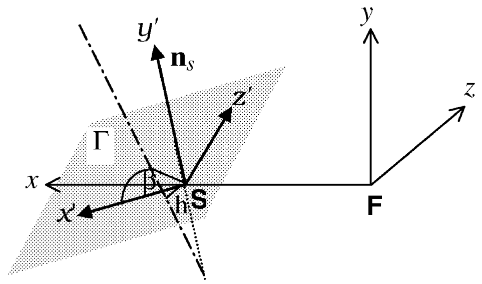

Fig. 4. The assistant coordinate system x'–y'–z' defined in x–y–z.

owed). The y'-axis coincides with the vector $\mathbf{n}_s$. The x'-axis is defined in the plane Γ along the intersecting line with the plane formed by the x- and y'-axis. Then the z'-axis is derived by applying the right-hand rule. This assistant coordinate system is shown in Fig. 4.

From Fig. 3 it is clear that the rotation of Ψ can be described by a rotation of the line $\mathbf{S}T$ (the distance from $\mathbf{S}$ to Ψ is h). The scanning angle of $\mathbf{S}T$ is $\beta = \beta_0 + \omega_s t_s$, where ω_s is the scanning frequency of the detecting plane Ψ and β_0 is the initial angle.

Firstly, the equation of the plane Ψ can be easily represented in the x'–y'–z' coordinate system. At any time, the normal unit vector of plane Ψ, denoted as $\mathbf{e}$, is expressed in x'–y'–z' coordinates as

$$\mathbf{e} = [\,\cos\theta\cos\beta, \quad -\sin\theta, \quad \cos\theta\sin\beta\,]^{\mathrm{T}}. \tag{2}$$

So, in the x'–y'–z' coordinates, the equation of the detecting plane Ψ is

$$\mathbf{x}'^{\mathrm{T}}\mathbf{e} = h, \tag{3}$$

where h and θ are the parameters defined in Fig. 3.

Defining the translation vector $\mathbf{L}$ as the vector pointing from $\mathbf{F}$ to $\mathbf{S}$, we use the transformation $\mathbf{x} = \mathbf{R}\mathbf{x}' + \mathbf{L}$ to represent the expression of (3) under the x–y–z coordinate system

$$(\mathbf{x} - \mathbf{L})^{\mathrm{T}}\mathbf{R}\mathbf{e} = h. \tag{4}$$

Substituting (1) into (4), we get

$$K = \frac{h + (\mathbf{R}^{\mathrm{T}}\mathbf{L})^{\mathrm{T}}\mathbf{e}}{(\mathbf{R}^{\mathrm{T}}\mathbf{q})^{\mathrm{T}}\mathbf{e}}. \tag{5}$$

Now we further derive the expressions of (5) in form of the system parameters. Denoting the three basic vectors of the coordinate system x'–y'–z' as ($\mathbf{v}_x$, $\mathbf{v}_y$, $\mathbf{v}_z$), the rotation matrix $\mathbf{R}$ can be expressed as $\mathbf{R} = [\mathbf{v}_x,\ \mathbf{v}_y,\ \mathbf{v}_z]$. According to the definition of the coordinate system x'–y'–z', we know that $\mathbf{v}_y = \mathbf{n}_s$, therefore

$$\mathbf{v}_y = \begin{bmatrix} n_x \\ n_y \\ n_z \end{bmatrix} = \begin{bmatrix} \sin\rho_1\cos\rho_2 \\ \cos\rho_1 \\ \sin\rho_1\sin\rho_2 \end{bmatrix}, \tag{6}$$

where ρ_1 and ρ_2 are the azimuth and elevation angles of $\mathbf{n}_s$ (see Fig. 5).

Because the axes of $\mathbf{n}_s$, x and x' are coplanar, we can derive the vector $\mathbf{v}_x$ from the following expression:

$$\mathbf{i} = \cos(\delta)\mathbf{v}_x + \sin(\delta)\mathbf{n}_s, \tag{7}$$

where $\mathbf{i}$ is the unit vector of the axis x, δ the angle between x and x' (see Fig. 6). Therefore,

$$\mathbf{v}_x = \frac{\mathbf{i} - \sin(\delta)\mathbf{n}_s}{\cos(\delta)} = \frac{1}{\cos(\delta)}\begin{bmatrix} 1 - n_x^2 \\ -n_x n_y \\ -n_x n_z \end{bmatrix}. \tag{8}$$

Here we have used the relations of $\mathbf{i} = [100]^{\mathrm{T}}$ and $\sin(\delta) = n_x$.

Finally, the vector $\mathbf{v}_x$ can be derived from $\mathbf{v}_z = \mathbf{v}_x \times \mathbf{v}_y$. From (8), we get

$$\mathbf{v}_z = \frac{1}{\cos(\delta)}(\mathbf{i} \times \mathbf{n}_s) = \frac{1}{\cos(\delta)}\begin{bmatrix} 0 \\ -n_z \\ n_y \end{bmatrix}. \tag{9}$$

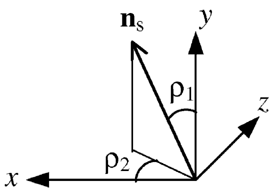

Fig. 5. Azimuth and elevation angles of $\mathbf{n}_s$.

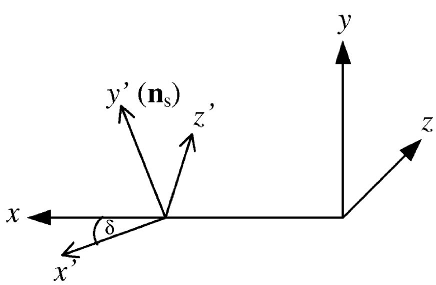

Fig. 6. Definition of the angle δ (x, y' and x' are coplanar).

Now the three basic vectors $(\mathbf{v}_x, \mathbf{v}_y, \mathbf{v}_z)$ have been formulated in terms of the parameters ρ_1 and ρ_2 through (6)–(9).

Denoting $\mathbf{q}' = \mathbf{R}^{\mathrm{T}}\mathbf{q}$, we can obtain the following results:

$$q'_x = \frac{1}{\cos(\delta)}(\sin\gamma\cos\alpha - \sin(\delta)q'_y),$$
$$q'_y = \frac{1}{\cos(\delta)}(\sin\rho_1\cos\rho_2\sin\gamma\cos\alpha + \cos\rho_1\cos\gamma + \sin\rho_1\sin\rho_2\sin\gamma\sin\alpha), \quad (10)$$
$$q'_z = \frac{1}{\cos(\delta)}(-\sin\rho_1\sin\rho_2\cos\gamma + \cos\rho_1\sin\gamma\sin\alpha),$$
$$\sin(\delta) = \sin\rho_1\cos\rho_2,$$
$$\cos(\delta) = \sqrt{1-\sin^2(\delta)}.$$

Denoting $\mathbf{L}' = \mathbf{R}^{\mathrm{T}}\mathbf{L}$, we obtain

$$L'_x = \frac{1}{\cos(\delta)}(L - \sin(\delta)L'_y),$$
$$L'_y = L\sin\rho_1\cos\rho_2, \quad (11)$$
$$L'_z = 0.$$

Expanding (5) in the form of

$$K = \frac{h + L'_x e_x + L'_y e_y}{q'_x e_x + q'_y e_y + q'_z e_z} \quad (12)$$

and combining (3), (10) and (11), the parameter K in (1) can be computed in terms of the system parameters.

4. Calibration method

Although the eight parameters involving in the computation of the measurement model are pre-designed in the mechanical construction, a calibration process is necessary to determine these parameters through real measurements. Unlike the CCD modality, point sensing of the system is finished in a time sequential way, so the calibration routine is different to those commonly used techniques for laser range finders existing in literatures (e.g. [4,12]). We proposed a new algorithm for the calibration of the laser beam-scanning triangulation system, by which the calibration is formulated as an optimal estimation of system parameter and the point correspondences are avoided. The system parameters are derived from the least-square estimation through a planar fitting routine. A novel feature of our approach is that the uncertainties in measurement are modelled in domain of sensing variable, rather than in the domain of *x–y–z* form. Because the errors of the output are treated with a refined description, the computation yields to reliable results in the sense of statistical optimisation.

4.1. Parameter estimation using a planar fitting algorithm

In general, reference objects/points are required as the ground truth to formulate the determined or over-determined equations by which the parameters can be derived. Simple and convenient point-matching algorithms for calibration are commonly based on the assumption that correspondence between the reference point and its measured counterpart has been identified. However, there exist difficulties in the standard point correspondence method. First, it is difficult to guarantee the known reference points being illuminated by the laser beam—they may lie in between the beam tracks in scanning process. Second, since the laser beam is not an ideal point pattern, there exists uncertainty in positioning of the target point. To derive the system parameter independently, only relative positions of the reference points are pre-known with respect to the defined coordinate system. Thus more uncertainties will be induced in forming the equation as constraints in calculating the relative positions.

To avoid the point correspondence problem, alternative solutions with co-linearity or coplanarity constraints have been used [6,12] for parameter determination. In notion of [12], we formulate the constraints using the plane-point correspondence and furthermore, configure the solution to an optimal estimation of an over-determined problem.

Suppose a point from an unknown plane is measured as $\mathbf{x}(\mathbf{a})$, where $\mathbf{a}$ denotes the system parameters, then the planarity constraint yields to $\mathbf{n}^{\mathrm{T}}\mathbf{x}(\mathbf{a}) = b$, where $(\mathbf{n}, b)$ describe the pose of the plane.

Besides the system parameters, also the parameters of the plane, stored in the vector $\mathbf{p} = (\mathbf{n}, b)^{\mathrm{T}}$, should be determined simultaneously. In other words, the planar constraint implies a posterior positioning of the measured points, which is also the elementary spirit used in the so-called self-calibration approaches [9,14].

Obviously, assume the parameters are known, three such constraints with three non-parallel planes give rise to a point measurement that is just the intersecting position of the three planes. It means that the plane-point correspondence can be interpreted as "indirect" point correspondence in an alternative manner. But the difficulties of direct point correspondence in measurement can be avoided.

To formalize the calibration as an estimation problem, we do as described below. Assume the system parameters represented by **a** are known, the plane parameters represented by **p** can be solved by minimizing a cost function that is defined to test the "goodness" of fitting data points to the plane.

Suppose the error of the measurement of a planar point **x**, denoted as $\Delta\mathbf{x}$, is independent identically distributed (i.i.d.) noise, then the distance of the measured point to the plane $d = \Delta\mathbf{x}^{\mathrm{T}}\mathbf{n}$, where **n** denotes the normal vector of the plane has also the same distribution. For a set of measured planar points, the function

$$D(\mathbf{a}, \mathbf{p}) = \sum_{i=1}^{m} d_i^2 \tag{13}$$

can be used to evaluate the variance of noise $\Delta\mathbf{x}$ as statistics.

Using a few planes in different poses as the calibration objects, the cost function can be defined as

$$\Theta(\mathbf{a}, \mathbf{p}_k) = \sum_{k=1}^{K} D_k, \tag{14}$$

where K is the number of the planes used for calibration, **a** and $\mathbf{p}_k$ $(k = 1, \ldots, K)$ are then derived by minimising the cost function of (14)

$$\frac{\partial\Theta}{\partial\mathbf{a}} = 0, \qquad \frac{\partial\Theta}{\partial\mathbf{p}_k} = 0, \quad \forall k = 1, \ldots, K. \tag{15}$$

Because the system parameters **a** are derived incorporating with the plane parameters from (15), the solution of (15) could be ill-posed, even if there are sufficient data points sampled from the plane. To avoid an ill-posed problem, at least three non-parallel planes should be used to generate the cost function (14), i.e., $K \geq 3$. Since three non-parallel planes determine a 3D point at their intersecting position, minimization of (14) means that the estimated system parameters **a** measure the squared error of this generated point being minimum.

It should be noted that the above formulation for the LSE solution of the system parameters is based on the assumption that the error of measurement in geometric domain, i.e. $\Delta\mathbf{x}$, is stationary i.i.d. noise. Unfortunately, this assumption is usually not correct in reality. To get a more reliable estimate of the parameters, we considered the physical sensing process to model the uncertainties in measurement in the domain of sensing variable. Thus a sensor-dependent calibration routine is proposed as describe below.

4.2. The sensor-dependent LSE solution

For the triangulation measurement system, the range measurement is indexed by angles, i.e. (α, β, γ), as illustrated in Section 3. As low-level sensing outputs, usually the error in the angle measurement can be simplified as a stationary stochastic process. Therefore, it is feasible to model the error of the input as a noise with normal pattern. However, after being converted to the *x–y–z* form, the errors represented in *x–y–z* coordinates usually do not preserve the properties in the original form of (α, β, γ). So the LSE criterion with the noise model in the *x–y–z* form will yield unreliable results.

Generally, such kind of error performance is shared by all triangulation measurement systems, in spite of alternatives in sensing patterns. To eliminate the influence of the non-linear mapping from the input sensing variables to the output *x–y–z* representation, estimation in system calibration should be established in the domain of the sensing variables, rather than the *x–y–z* form.

For the laser beam-scanning measurement system, the scanning angles are determined by measuring the scanning time t_{f}, t_{s}, and t_{l}. In the implementation of the calibration, points on a plane are manually selected, that is, t_{f} and t_{s} are pre-determined to position the instantaneous pose of the laser beam and the corresponding t_{l} positioning the instantaneous detecting plane is recorded in the scanning process for each selected object point. Therefore, only the error of t_{s}, denoted as Δt_{s} and thought to be with constant variance, is involved in the computation.

Given system parameters **a**, the coordinates of a measured point can be expressed in the form

$$\mathbf{x} = \mathbf{X}(\mathbf{a}, t_l, t_f, t_s).$$

In first-degree approximation, errors in the coordinates can be expressed as

$$\Delta\mathbf{x} = \frac{\partial\mathbf{X}}{\partial t_s}\Delta t_s. \tag{16}$$

Suppose **x** is measured from a planar point. Then the error will be

$$\mathbf{n}^{\mathrm{T}}\Delta\mathbf{x} = \mathbf{n}^{\mathrm{T}}\left(\frac{\partial\mathbf{X}}{\partial t_s}\right)\Delta t_s \tag{17}$$

define

$$w = \left[\mathbf{n}^{\mathrm{T}}\left(\frac{\partial\mathbf{X}}{\partial t_s}\right)\right]^{-1} \quad \text{and} \quad d = \mathbf{n}^{\mathrm{T}}\Delta\mathbf{x},$$

Δt_s can be written as $\Delta t_s = wd$. Therefore, Δt_s can be interpreted as the "weighted" distance of d with respect to the function of (13).

Given a set of planar points, the statistics of the error Δt_s can be formulated as

$$\tilde{D}(\mathbf{a}, \mathbf{p}) = \sum_i w_i^2 d_i^2. \tag{18}$$

Assuming the total number of the test plane objects is K, the corrected cost function for calibration is

$$\tilde{\Theta}(\mathbf{a}, \mathbf{p}_k) = \sum_{k=1}^{K} \tilde{D}_k. \tag{19}$$

Minimising the cost function of (19) can be carried out with numerical methods.

This algorithm was applied to calibrate the laser beam-scanning ranging system as mentioned in Section 2. The results are shown in Table 1. The point sets were sampled from a thin wooden plate (size 280 mm × 140 mm) at three different poses within a range 0.5–1 m along the z-direction. The variance in measurements of t_s and distance, denoted as $\overline{\Delta t_s^2}$ and $\overline{d^2}$, were estimated by the residue of $\sum_i(\Delta t_{s,i})^2$ and $\sum_i(d_i)^2$ and the number of points, respectively. The gradient-descending numerical method was applied to minimize the cost function of (19). The initial estimate of the parameters was determined from the designed value of the mechanical system construction. The convergence was reached after 8–10 iterations.

Table 1
Results of the calibration of the laser beam-scanning system[a]

α_0	2.7615
β_0	0.9350
γ_0	1.7870
ρ_1	0.0784
ρ_2	2.4890
h	0.2714
θ	0.8767
L	65.818
$\overline{\Delta t_s^2}$ (s)	3.3143×10^{-6}
$\overline{d^2}$ (cm)	1.0630

[a] Parameters were defined in Section 3. Total number of sampled points is 500.

A prototype of the system has been implemented for 3D measurement, which has been used in the research project of man-made object recognition from range data [13]. Fig. 7 shows an example of the collected surface data points of a real object (a cup) obtained with the system. The object was located at a distance of about 1 m from the system and the sensing time (t_f, t_l and t_s) was recorded for each sensed surface point. The plotted points were showed in x–y–z form after computation using the system parameters obtained with the calibration method. These 3D data have been used with surface fitting algorithm in the module of object recognition [13]. The average squared distance from the data point to the corresponding object surface was estimated as about 0.9 cm^2, which is the same order of the computed $\overline{d^2}$ in Table 1.

The errors in calibration measurement were mainly caused by the systematic errors of the described system, i.e., the imperfect performances of the optical and electronic elements as well as mechanical implementation. Briefly, the major causes of errors include:

- *Uncertainty in recording of the scanning time*. In contrast to CCD imaging, the output of this system is the recorded scanning time (t_l, t_f, t_s) at which a point is sensed. Although the clock frequency of the time counter is high enough (about 10 MHz), there exist uncertainty at the moment to trigger a time counting process in each scanning periods, for that the triggering signal is not an ideal pulse in electronic realisation. Of course, improvement in circuit implementation can reduce such kind of errors.
- *Expansion of the laser point-beam*. Due to the intrinsic divergence of the laser beam, ambiguity

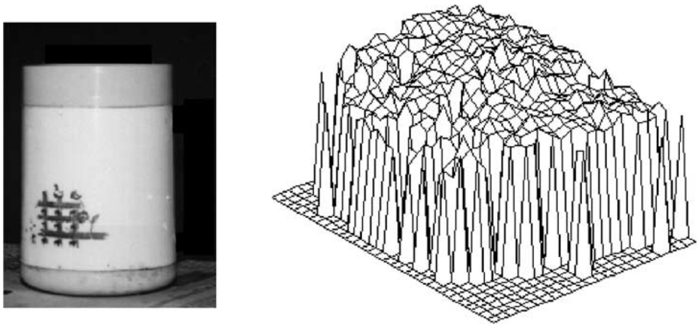

Fig. 7. A cup and its measured surface points using the implemented laser beam-scanning triangulation measurement system. Here the cup was shown in grey-level image and the 3D surface points were plotted with Mathcad.

in positioning an object point is inevitable, which yields uncertainty in determination of the scanning angles. This problem becomes significant when the laser beam hits the object surface oriented around the projecting direction of the laser beam. In fact, in data acquisition using the implemented system, as the example of Fig. 7, larger errors occurred near the boundary of the object.

- *Thickness of the detecting slit*. The point detection was realized by imaging a slit through a rotating mirror onto the scene, as illustrated in Fig. 2(b). The slit is located at the focus of a lens so that an image of the detecting plane performs the scanning process. Due to non-ideal focus location, the imaged "thickness" of the detecting plane could be expanded, which causes uncertainty in determination of the angle β. Only improvement of optical implementation is expected to suppress such error.
- *Instability of scanning frequencies*. The precision of the scanning frequencies is no doubt very important for the accuracy of laser beam-scanning measurement. Any instability of the motor rotation will induce errors in the computation of the scanning angles. The solution of this problem relies on the improvements of rotating modality used for the scanning measurement.

5. Conclusions

This paper proposed a practical approach to model and to calibrate the laser beam-scanning triangulation measurement system. Unlike most published range finder, the described system performs a beam illumination patter with a two-dimensional scanning mechanism and a slit-scanning detection. Without the CCD camera, the point sensing is process with an independent photo-electronic transducer through a time sequential way. By recording the three scanning angles at which an object point is sensed, 3D position of the point is calculated through the triangulation algorithm. The coordinate system fixed to the measurement system was modelled and the formulation of 3D computation was described.

The system parameters, defined with the measurement model, were determined through calibration. To avoid the difficulties in point correspondence, we proposed a new approach for parameter estimation using a planar fitting algorithm. In general, this algorithm can be extended to solve the calibration problem for the triangulation measurement system in the sense of optimal estimation. The novelty of our approach is that the solution is obtained with a refined sensor-dependent formulation. Considering that the non-linear transformation from the sensing variable to the x–y–z representation leads to the degeneration of the statistics of the sensing output, we modelled the uncertainties of measurement in the domain of the sensing variable, the output of time recording in the scanning process. Because the errors occurred in the sensing output is thought to be adapt to an additive noise model, the determination of the system parameters was expected to be optimal as the LSE solution formulated in the domain of sensing variable. The results of the calibration with respect to the system introduced in this paper and an analysis of causes of errors were given.

References

[1] A. Basu, Active calibration of cameras: Theory and implementation, IEEE Transactions on Systems, Man and Cybernetics 25 (1995) 256–265.
[2] P.J. Besl, Active, optical range imaging sensors, Machine Vision and Applications 1 (1988) 127–152.
[3] R.C. Bolles et al., Projector camera range sensing of three-dimensional data, Machine Intelligence Research Applied to Industrial Automation, SRI International, Menlo Park, CA, 1983, pp. 29–43.
[4] Y.Y. Cha, D.G. Gweon, A calibration and range-data extraction algorithm for omnidirectional laser range finder of a free-range mobile robot, Mechatronics 6 (6) (1996) 665–689.
[5] G. Champleboux et al., Accurate calibration of cameras and range imaging sensors: the NPBS method, in: Proceedings of the IEEE International Conference on Robotics and Automation, Nice, France, 1992, pp. 1552–1557.
[6] C.H. Chen, A.C. Kak, Modeling and calibration of a structured light scanner for 3D robot vision, in: Proceedings of the IEEE Conference on Robotics and Automation, Raleigh, NC, 1987, pp. 807–815.
[7] F. Du, M. Brady, Self-calibration of the intrinsic parameters of cameras for active vision system, in: Proceedings of the IEEE Conference on Computer Vision and Pattern Recognition, 1993, pp. 477–482.
[8] O.D. Faugeras, O.T. Luing, S.J. Maybank, Camera self-calibration: Theory and experiments, in: Proceedings of the European Conference on Computer Vision, 1992, pp. 321–334.
[9] S.D. Ma, A self-calibration technique for active vision system, IEEE Transactions on Robotics and Automation 12 (1996) 114–120.
[10] T.H. Moring, Acquisition of three-dimensional image data by a scanning laser range finder, Optical Engineering 28 (8) (1989) 897–902.
[11] N.E. Pears, Active triangulation range finder design for mobile robots, in: Proceedings of the IEEE/RSJ International Conference on Intelligent Robots and Systems, Vol. 3, 1992, pp. 2047–2052.
[12] I. Reid, Projective calibration of a laser-stripe range finder, Image and Vision Computing 14 (1996) 659–666.
[13] G.Y. Wang, Recognition of man-made objects from range data, Ph.D. Thesis, University of Twente, 2000. ISBN 90-365-14452.
[14] G.Q. Wei, K. Arbter, G. Hirzinger, Active self-calibration of robotic eyes and hand-eye relationships with model identification, IEEE Transactions on Robotics and Automation 14 (1) (1998) 158–166.
[15] G. Zheng et al., Laser difference frequency scanning 3-D vision sensing system for underwater robot, in: Proceedings of the Intervention ROV'91, 1991, pp. 90–96.

Guoyu Wang was born in Qingdao, China, on 27 January 1962. He received the B.Sc. and M.Sc. degrees in Physics in 1984 and 1987, respectively, from the Department of Physics, Ocean University of Qingdao, China. He has been working in the Department of Physics and then in the Department of Electrical Engineering, Ocean University of Qingdao since 1987. During 1993–1994 and 1990–2000 he did research as a visiting scholar in the Department of Electrical Engineering, University of Twente, The Netherlands, and obtained the Ph.D. degree in University of Twente in 2000. His current research interests include pattern recognition, image analysis and machine vision.

Bing Zheng was born in Qingdao, China on 7 November 1968. He received the B.Sc. and M.Sc. degrees in 1987 and 1995, respectively, from the Department of Electrical Engineering, Ocean University of Qingdao. Since 1988 he has been working in the Department of Electrical Engineering, Ocean University of Qingdao, and now he is working towards his Ph.D. degree. His major research subjects are 3D vision and image-based measurement systems.

Xin Li was born in Qingdao, China on 27 January 1959. He received the B.Sc. degree in 1981 from the Department of Electrical Engineering, Zhejiang University, China. Subsequently, he worked in the Department of Electrical Engineering, Ocean University of Qingdao. He is currently a professor in the Department of Electrical Engineering, Ocean University of Qingdao. His research interests include signal processing, robotics and machine vision.

Zweitze Houkes was born in Utrecht, the Netherlands, on 30 October 1939. He has been an associate professor of Computer Vision at the Department of EE of the University of Twente since 1984. He retired in November 2001. He received his M.Sc. in Electrical Engineering from Delft University of Technology, The Netherlands, in 1963 and his Ph.D. in 2000 at the University of Twente. Before 1968 he worked for Philips Telecommunication, then for the Dutch Railways on signalling and automatic train control. In 1968 he joined the Electrical Engineering Department of the University of Twente, where he was engaged in research on optimal control and estimation in the Measurement and Instrumentation Laboratory and in Control Engineering. He is a senior member of IEEE and member of IAPR.

Paul P.L. Regtien received his M.Sc. degree in 1970 and the Ph.D. degree in 1981, both from Delft University of Technology, The Netherlands. From 1981 to 1982 he was with Endress und Hauser, Germany, where he developed a new high-temperature humidity measurement system for industrial use (two patents). Returned to Delft University of Technology, he managed several research projects on robotic sensors and instrumentation. Since 1994 he is a full professor at the Twente University, Faculty of Electrical Engineering, The Netherlands, and head of the Laboratory for Measurement and Instrumentation. Present research activities are measurement science, imaging (optical, acoustic, tactile), mechatronics, sensor technology and instrumentation.

He is a board member of the IOP journal *Measurement Science and Technology*, Chairman of TC1 (Education and Training in Measurement and Instrumentation) of IMEKO, member of TC17 (measurements in Robotics) of IMEKO, member of the Eurosensors International Programme Committee, member of the Institute of Physics (UK) and Senior member of the IEEE.